Low platinum fuel cell as enabler for the hydrogen fuel cell vehicle

Journal of Power Sources 598 (2024) 234140

Contents lists available at ScienceDirect

Journal of Power Sources

journal homepage: www.elsevier.com/locate/jpowsour

Low platinum fuel cell as enabler for the hydrogen fuel cell vehicle

Tatiana Santos Andrade *, Torbjörn Thiringer

Department of Electrical Engineering, Chalmers University of Technology, Gothenburg, Sweden

HIGHLIGHTS

- Emerging catalysts of low-loading Pt fuel cells were modeled to fuel cell systems.
- The systems were inserted in a vehicle powertrain, and simulated for a driving cycle.
- Higher efficiencies than a commercial fuel cell vehicle were obtained.
- The high vehicle performance was related to the fuel cell load during the drive cycle.
- The results support cost-efficient fuel cell vehicles by reducing the platinum loading.

ARTICLE INFO

Keywords:
Hydrogen strategy
Fuel cell vehicles
PEM fuel cell
Fuel cell system
Automotive
PGM catalysts

ABSTRACT

In this work, the design and modeling of a fuel cell vehicle using low-loading platinum catalysts were investigated. Data from single fuel cells with low Pt-loading cathode catalysts were scaled up to fuel cell stacks and systems, implemented in a vehicle, and then compared to a commercial fuel cell vehicle. The low-loading Pt systems have shown lower efficiency at high loads compared to the commercial systems suggesting less stable materials. However, the analysis showed that the vehicle comprising low-loading Pt catalysts achieves similar or higher efficiency compared to the commercial fuel cell vehicle when being scaled up for the same number of cells. When the systems were scaled up for the same maximum power as the commercial fuel cell vehicle, all the low-loading Pt fuel cell systems showed higher efficiencies. In this case, more cells are needed, but still, the amount of Pt is significantly reduced compared to the commercial one. The high-efficiency results can be associated with the vehicle's power range operation that meets the region where the low-loading Pt fuel cells have high performance. The results suggested a positive direction towards the reduction of Pt in commercial fuel cell vehicles supporting a cost-competitive clean energy transition based on hydrogen.

1. Introduction

Platinum is pointed out as responsible for about 40–55% of the total cost of the stack fuel cell, which makes its reduction highly necessary for the breakthrough of cost-effective fuel cell vehicles (FCVs) [1–4]. Due to the low kinetic of the oxygen reduction reaction that takes place in the cathode, the current Pt-loading on that electrode is the critical design part accounting for about 85% of the total platinum of the fuel cell stack [5–8]. However, designing no or low-loading Pt cathodes is still challenging, requiring specialized strategies to achieve enhanced variations toward the electrochemical surface area and oxygen transport. While Pt-free cathodes still seem far off to be an alternative to state-of-art electrodes due to their low performance and poor stability [3,9–11], novel promising low-loading Pt catalysts have been reported using different approaches such as chemical modification and dry methods (e.g. physical vapor deposition). While the dry approaches have been showing many advantages in controlling size and morphology deposition, some chemical-designed catalysts are highlighted due to their high performance [1,12]. Those catalysts outstand DOE's (U.S. Department of Energy) targets and protocols regarding performance and stability in the operation of a single fuel cell for transportation applications indicating their suitability to be applied in an FCV lifetime operation [4]. For instance, Chong and collaborators have reported a catalyst composed of Pt–Co nanoparticles over a Pt–free substrate with a Pt-loading as low as 0.033 mg/cm^2 [13]. More recently, Lee and collaborators reported a channeled mesoporous carbon with Fe and Pt with Pt loading as low as 0.01 mg/cm^2 which corresponds to the highest performance per mass of Pt reported so far to the best of our knowledge [12]. In terms of Pt

* Corresponding author.
E-mail address: tatianas@chalmers.se (T.S. Andrade).

https://doi.org/10.1016/j.jpowsour.2024.234140
Received 24 November 2023; Received in revised form 17 January 2024; Accepted 26 January 2024
Available online 13 February 2024

loading, those catalysts achieved a reduction of 89–97% compared to the total Pt-loading on the stack presented in a commercialized fuel cell vehicle, i.e., Toyota Mirai (0.31 mg-Pt/cm^2). Thus, low-loading Pt catalysts have demonstrated attractive results in replacing the state-of-the-art electrodes in fuel cells aimed at automotive applications. However, translating the single-cell results for a vehicle application regarding its efficiency for a driving cycle is usually beyond the scope of novel material studies.

Analysis regarding scaling up from single fuel cells to stacks followed by performing experiments in FCVs might be costly and complex. Therefore, the modeling of such systems is an alternative step to evaluate the impact of low-loading Pt catalysts to be inserted in emerging FCVs. Recently, Ahluwalia and collaborators have modeled fuel cell systems with reduced amounts of platinum for driving cycles. In this study, catalysts with Pt loading from 0.1 to 0.2 mg/cm^2 were scaled up to fuel cell stacks, and evaluated regarding the limits of their operating conditions to be inserted in FCVs without compromising the fuel cell durability [14]. While that approach was valuable in analyzing the potential of the state-of-art electrodes with a reduced amount of Pt to be employed in FCVs, it does not consider the emerging nanotechnologies that demonstrated high stability even with lower loading Pt (up to 0.035 mg/cm^2). To the best of our knowledge, there is a knowledge gap regarding the performance of low-Pt fuel cell systems and their relation to commercial Pt fuel cell systems in a vehicle.

Therefore, in this work, we present an investigation addressing the implementation of emerging nanotechnologies of stable and high-performance low-loading Pt cathodes on the efficiency of an FCV for a driving cycle. Thus, the purpose of this work is to approximate the nanotechnology development regarding fuel cells to their application for automotive propulsion, contributing to a green energy transition based on hydrogen. In this regard, some specific contributions of this work are.

- Scaling up single fuel cells using promising low-loading Pt catalyst combined with data of a commercial FCV considering two models: 1) the same number of cells; or 2) the same maximum power.
- Evaluation of the power-efficiency curves constructed with the ones of a commercial FCV considering homogenous mass and heat transfer (no losses regarding scaling from the single cell to stack) and heterogenous mass and heat transfer.
- Determination of each powertrain component loss contribution followed by the vehicle powertrain efficiency during the drive cycle using research data, and mathematical models for an FCV comprising a fuel cell with low, or commercial standard loading Pt catalyst.

2. Methods

In this work, experimental data of single fuel cells were modeled as stacks and systems and then utilized in a simulation of an FCV for a driving cycle. To describe the methods implemented, this section is divided into 5 sub-sections. The first subsection, *fuel cell selection*, refers to the experimental data that was used as reference: single-cell experimental data using low-loading Pt catalysts (polarization curves) and the experimental data of a fuel cell of a commercial FCV using high-loading Pt catalyst (efficiency-power curve). The second subsection, *fuel cell stack and system model*, refers to the modeling description of the scaling-up of the single cell to stacks and systems. Thus, after the scaling-up modeling, the novel fuel cells could be compared with the commercial fuel cell data. Finally, the last three subsections, *system model set-up*, *battery* and *control strategy*, refer to the FCV modeling and simulation that was implemented using the modeled fuel cells or the commercial fuel cell data as the fuel cell model.

2.1. Fuel cell selection

To model the low-loading Pt fuel cells, research experimental data of single fuel cells that meet DOE's technical target for transportation applications, e.g. mass activity (>0.44 A/mg-Pt) and stability protocols (>5000 h with cycling) was considered. The Pt loading for the selected data was in the range of 0.01–0.035 mg/cm^2. Four catalysts were selected, two with 0.033–0.035 mg-Pt/cm^2 and two with 0.01 mg-Pt/cm^2. All experiments of the selected data were performed at 80 °C using H_2-air as the stream in a 5 cm^2 cell. The first two are catalysts consisting of platinum-cobalt core-shell nanoparticles in a platinum-free catalytic substrate with slightly different Pt loading and the last two are channeled-mesoporous carbon (CMC) particles with PtFe with slightly different channel porous. Different strategies that demonstrated variations in the electrochemical surface area and mass transport were obtained. For the first two samples, the layer composed of Co strongly binds with the Pt nanoparticles and the Pt-free support, promoting the exposure of the Pt surface and facilitating electron and mass transport. For the other two samples, the high large surface area channels in the *C*-shell that encapsulate the PtFe nanoparticles are associated with both the high electrochemical surface and high mass transport of the catalyst. Detailed information related to the electrode synthesis can be found elsewhere, referred to as LP@PF-1, LP@PF-2, and CMC63-PtFe and CMC40-PtFe [12,13]. In this work, these materials are going to be referred to as E1 - 3.3 Pt, E2 -3.5 Pt, E3 - 1.0 Pt, and E4 - 1.0 Pt. To differentiate the Pt sampling loading, E1 and E2 are referred to in this work as low-loading Pt catalysts while E3 and E4 as ultra-low-loading Pt catalysts. The polarization curves of the selected cells are shown in Fig. 1A. Those curves were used to scale up to stack level and to be implemented in the fuel cell system. For comparison purposes, the stack and system of a commercial FCV, i.e. Toyota Mirai, published in Ref. [16], was used. The fuel cell stack of the commercial vehicle is composed of 370 cells with an area of 237 cm^2, a maximum power of 114 kW, and a cathode Pt loading of 0.31 mg/cm^2 [7,8,15]. The stack and system efficiency curves for the vehicle used as reference are shown in Fig. 1B. The first part of the curve (<6 kW) in Fig. 1B, where the efficiencies present lower values for low power values can be attributed to the activation loss area [16]. Since the fuel cell operation should be favored in the ohmic region and avoided in the activation loss area, a minimum of 6 kW of power (P_{minFC}) was also assumed for the operation of all the modeled stacks and systems.

2.2. Fuel cell stack and system model

To implement the selected single-cell profiles in the vehicle powertrain, the measurements results shown in Fig. 1A were scaled up to power-efficiency curves modeled with the size of the commercial fuel cell vehicle shown in Fig. 1B. For that, first, the selected single-cell curves previously described were modeled in series considering the area per cell as in the commercial fuel cell (237 cm^2) to form the stack. Two models were proposed for the stack: 1) Model 1: the same stack size (370 cells), and 2) Model 2: with the same maximum power (114 kW). Thus, the current (i_{stack}), the voltage (V_{stack}) and the power (P_{stack}) used for the stack curve can be summarized as a function of the number of cells (NCs), the current (i_{sFC}), and the voltage (V_{sFC}) of the single cells as

$$i_{stack} = i_{sFC} * 237 \quad (1)$$

$$V_{stack} = V_{sFC} * NCs \quad (2)$$

$$P_{stack} = V_{stack} * i_{stack} \quad (3)$$

Where NCs is 370 for model 1 and the P_{stack} is 114 kW for model 2. Thus, when the same stack size is designed, the cells have different power capacities, while when maximum power is standardized, i.e. more cells are needed for those whose maximum power efficiencies are lower. Furthermore, to scale up from single cells to stack, losses associated with heterogenous heat and mass transfer (e.g. temperature distribution, oxygen transport, and water production) are usually related to the struggle to keep the same conditions all over the stack, especially at

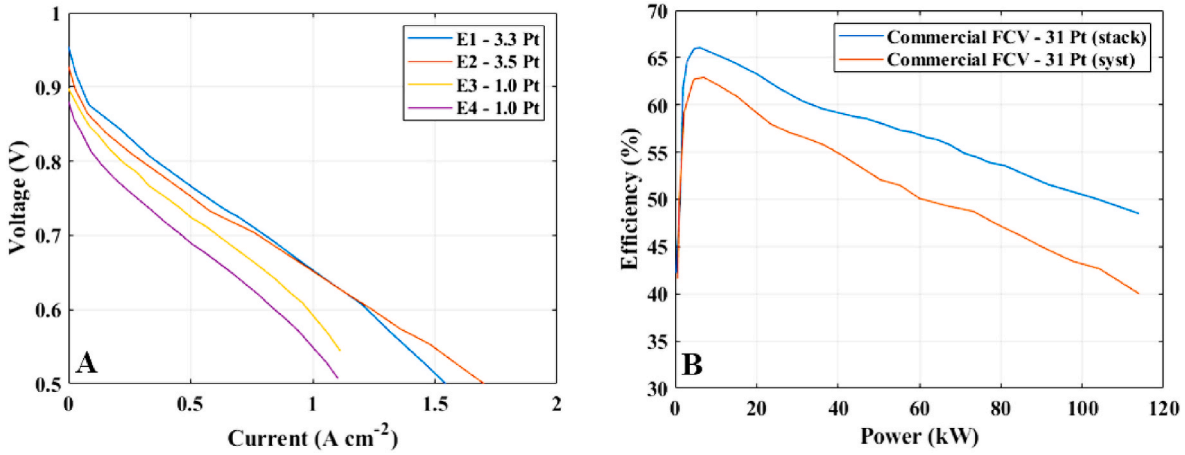

Fig. 1. Measured Polarization curves for single cells using novel materials with low Pt loading (A) and stack and system fuel cell efficiency curves from a commercial FCV (B).

higher power demand. Scaling-up investigations have reported varied efficiency flaws that could be minimized or even reported as negligible if an efficient control distribution is employed [17–22]. Therefore, in this model, two considerations regarding this issue were considered: 1) homogenous heat and transfer losses, meaning no extra losses were included regarding scaling up from single cells to stack, and 2) heterogeneous mass and heat transfer issues which included a linear increased power loss in the range of 0–8% losses up to the maximum power, based on previous scaling-up investigations reports [19,22]. Considering 1.23 V as the theoretical maximum output for a fuel cell, the efficiency curve values for the fuel cell stacks (ef_{stack}) for homogeneous and heterogenous heat and transfer losses as a function of the single fuel cell voltage were calculated as

$$ef_{stack,homo} = 100 * \frac{V_{sFC}}{1.23} \tag{4}$$

$$ef_{stack,hetero} = ef_{stack,homo} * \left(1 - \frac{P_{stack}}{P_{stack,max}} * 0.08\right) \tag{5}$$

Besides the fuel cell stack, the fuel system is also composed of the pumps, the compressor, and the converter. To account for the losses in the system, related to the compressor, water pump, and converter, reported data from a commercial FCV, as shown in Fig. 1B, was used [16]. As shown in the figure, the loss in the system is strongly related to the power that comes from the fuel cell. Thus, higher power demand lowers the efficiency of the other components, especially, the compressor, showing a maximum of 17% efficiency losses at its maximum power operation point. Therefore, considering the same proportion reported with a linear loss in the range of 0–17%, the efficiency curve for the system was calculated as

$$ef_{system} = ef_{stack} * \left(1 - \frac{P_{stack}}{P_{stack,max}} * 0.17\right) \tag{6}$$

2.3. System model set-up

The FCV powertrain was designed considering the following components: 1) the wheels which are related to the car model and its dynamics; 2) the gear which transmits energy from the electric motor to the wheels; 3) the electric motor (EM) coupled with the inverter which converters DC (direct current) from the energy source (battery or fuel cell) into AC (alternate current) and converts electrical energy in mechanical energy to the gear; 4) the battery which can both provide DC to the EM through the inverter or take DC that comes from the EM/inverter when the vehicle is braking, and 5) the fuel cell system which can provide DC to the EM or the battery and it comprises the fuel cell, converter, compressor, and water pump. This system diagram described is shown in Fig. 2 and has been designed, modeled, and simulated using MATLAB software. The simulation was conducted in a backward scheme (the energy flow was considered from the drive speed target to the energy source) using the Worldwide Harmonized Light Vehicles Test Procedure (WLTP) cycle as the driving cycle reference. This WLTP is divided into 4-speed regions (low, medium, high, and extra-high) and was developed based on real-driving data [23]. The simulations have begun considering that the battery is charged to 90%, and all the powertrain components were simulated in an electrical steady state. The wheels, the gear, the motor, and the inverter were simulated as previously described but for a 2000 kg vehicle with a cross-sectional area of 2.3 m^2 [24]. Meanwhile, the fuel cell model was described in the previous section, and the battery and the control strategy used in this work are described in the following sections.

2.4. Battery

The battery model was implemented considering experimental data from a commercial pouch-cell lithium-ion battery previously reported in Refs. [25,26] with capacity and resistance scaled to meet a power-optimized battery of an FCV vehicle as further described. The battery operation was assumed to be in the range of 20 and 95% SOC with a 4 A h capacity and 6 mΩ resistance. Further, a total of 100 cells

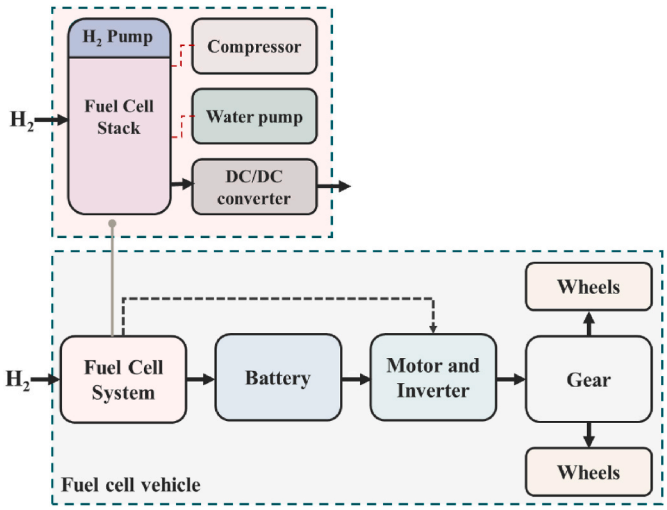

Fig. 2. System diagram for a fuel cell vehicle.

were connected in series and the maximum battery power was assumed to be 24 kW. Its capacity and maximum power values were chosen based on a commercialized fuel cell car that employs a lithium-ion battery, i.e., Hyundai ix35 [27]. The maximum *C*-rate (related to the battery speed of charge/discharge) was chosen based on its maximum power combined with data from the commercial power-optimized lithium-ion cells (26, 650) from LithiumWerks [28]. As follows, the maximum *C*-rate pulse was assumed to be 14 C and 8 C for the discharging and charging process, respectively. The parameters used are described in Table 1. The battery losses were calculated as a function of its current and resistance.

2.5. Control strategy

Since an FCV has two energy sources: a battery and a fuel cell, a control was needed to split the power between them. Some considerations might be highlighted further at this point. Only the battery can store energy that comes from the motor in case of deacceleration, but the storage was limited to its maximum charging rate as well as its maximum capacity. Moreover, the battery had limitations regarding its maximum discharge which was related to its maximum power. The maximum rates were described in the battery section. Both discharging and charging processes were also limited regarding the SOC operation of the battery, 20 and 95%, as previously mentioned. Likewise, the fuel cell had limitations, especially related to its minimum power which was related to the activation region area.

As follows, the control strategy proposed here had as input the power demand (P_{dem}) that needs to enter the inverter, the SOC as the measured variable, and the fuel cell minimum power as a constant (P_{minFC}). If the power demand was negative (the car is deaccelerating) the energy would come from the motor to the battery limited by the battery charging rate and SOC lower than 95%. For positive power demand and a SOC higher than 80, the battery was the main energy source but was limited to its maximum discharge. If the maximum discharge is reached, the fuel cell starts at its minimum. If the SOC was between 20 and 80%, the fuel cell and the battery would split the power as a linear function of SOC. In this case, as high as it was the SOC less power it would be taking from the fuel cell, respecting the limitations of the fuel cell and the battery accordingly. If the SOC was below 20%, the fuel cell would provide power to both the motor and to charge the battery.

3. Results and discussion

3.1. Model 1: same fuel cell stack size

For the fuel cell stack model 1, where the same stack size was assumed (370 cells), the curve profiles obtained for the scaled-up from single cells to stack and system of the samples E1-E4 have shown a higher declination compared to the commercial FCV stack, previously shown in Fig. 1B. Thus, when a relation of power (product of voltage and current) is established, it emphasizes the high variation in efficiency at high power values for samples E1-E4. The more dramatic drop if compared to the commercial FCV stack indicates that these materials demonstrated less stable performance at different power ranges. This profile might be associated with the reduced amount of Pt, a reasonable conclusion considering the higher performance of the low-loading Pt catalyst single cells (E1-E2) compared to the ultra-low-loading Pt ones (E3-E4). This observation agrees with previous investigations on low-loading Pt catalysts that have reported that those catalysts have limited performance that prevents their high efficiency, especially at high current densities [29,30]. The curves are shown in Fig. 3A–D for the case of homogeneous heat and mass transfer. The direct comparison with the fuel cell system of the commercial FCV can be found in Fig. 4A and B, considering, respectively, homogenous and heterogenous heat and mass transfer, as further described.

Thus, another outcome from Fig. 3A–D and Fig. 4A and B is the maximum power range relying on lower values if compared to the commercial FCV. The maximum power is in the range of 49–77 kW for the systems comprising low Pt loading catalysts (E1-E4). These values are considered to have an 8% lower variation and slightly more declination if accounting for the heat and mass transfer losses due to the higher challenge for a homogenous temperature and mass distribution at high power and the higher water production that hinders proper water management. Since the fuel cell stack for the commercial FCV has a maximum power of 114 kW for the same stack size, it can already be inferred that the fuel cells with ultra-low or low-loading Pt reach a maximum power that corresponds at their best of only 52% of the commercial FCV stack. However, when comparing the whole curve of the modeled samples with the commercial FCV system, shown in Fig. 4A and B, it can be observed that at lower power the fuel cell systems comprising low-loading Pt catalysts (E1-E4) presented a higher efficiency than the commercial FCV fuel cell system. Similar observations are also reported in Refs. [28,29], that associated low-loading Pt catalysts with high electrochemical performance but limited stability and efficiency at high power. Furthermore, for a power range lower than 40 kW, all the fuel cells presented a linear efficiency profile making the assumption that they would operate in the ohmic loss region reasonable. Thus, even though these materials still seem to lack stability for a broad power range compared to the commercial option, they might be promising alternatives if used in a limited power range. This limitation can be overcome by increasing the maximum power, as will be further discussed.

Table 1
Battery parameters.

Parameter	Value (unit)
Battery capacity	4 (Ah)
Battery cell resistance	6 (mΩ)
Number of cells	100 (−)
SOC range	20–95 (%)
Maximum power	24 (kW)
Maximum *C*-rate pulse discharge	14 (C)
Maximum *C*-rate pulse charge	8 (C)

3.2. Model 2: same maximum power

For the fuel cell stack model 2, where the same maximum power is considered (114 kW), the number of cells for each of the samples has to be increased since, as discussed in the previous section, these fuel cells presented lower maximum power compared to the commercial FCV. Thus, to reach the same maximum power as the commercial FCV, the number of cells should be increased by 50–130%. In the case where heterogenous heat and mass transfer are considered, at least an increase of 60% in the number of cells is needed to reach the same power. The visualization of the increased of cells compared to the commercial FCV for each of the samples E1-E4 can be seen in Fig. 5.

Despite the increase in the number of cells, for this model, all the samples comprising both ultra-low and low Pt loading (E1-E4) have shown higher efficiency for almost the whole power range compared with the commercial FCV (at least up to 80 kW), as shown in Fig. 6. Furthermore, if just the Pt amount is considered, even with the increased number of cells, the samples would still represent a Pt reduction of 81, 82, 93 and 92% compared to the commercial FCV for samples E1-E4, respectively. Thus, a great cost saving could be done since the systems considered could reach a Pt mass reduction of 81–97% lowering the stack cost by about 27–45%. Although other possible affected parameters were not considered in this work, such as more losses related to heterogeneous heat and mass transfer and the addition of other fuel cell components, our analysis is still representative due to the following reasons. The amount of platinum is considered to be the bottleneck for the spread commercialization of fuel cells. Further, losses related to heat and mass distribution mainly affect high power points which would be less relevant for the vehicle performance as will be discussed in the

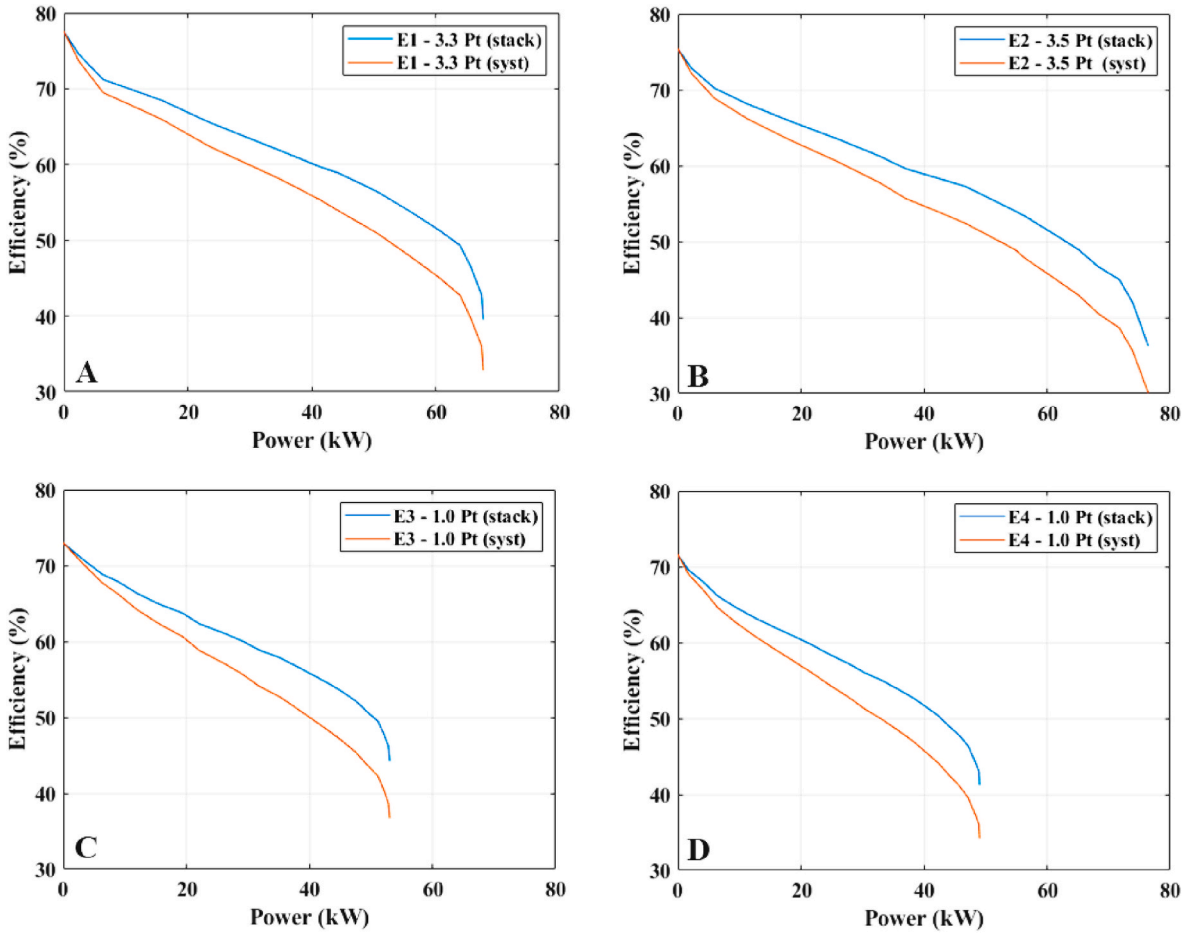

Fig. 3. Fuel cell stacks (blue curve) and systems (red curve) comprising 370 cells of the single cell samples E1-E4 (A–D). (For interpretation of the references to colour in this figure legend, the reader is referred to the Web version of this article.)

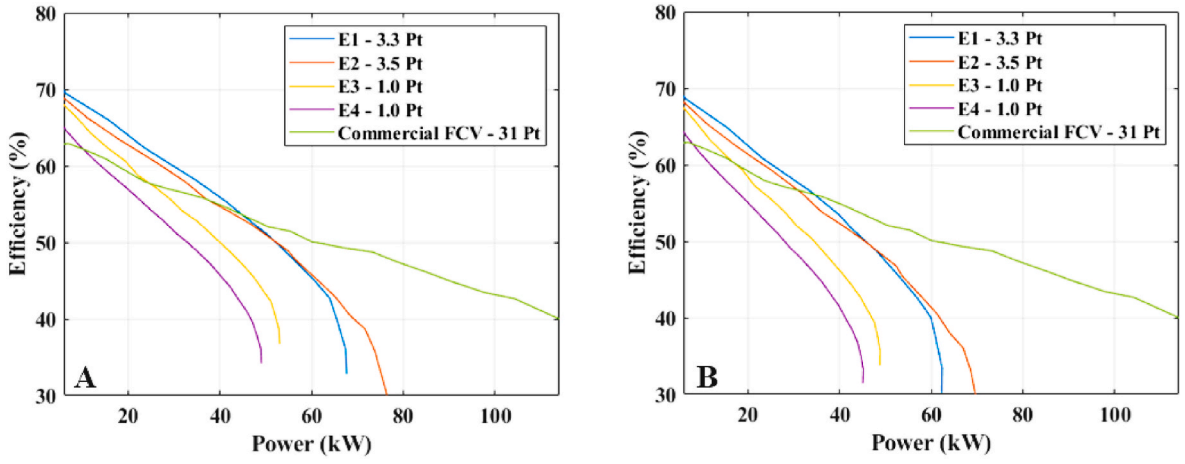

Fig. 4. Fuel cell systems comprising 370 cells of the single cell samples E1-E4 with low and ultra-low Pt loading compared with the fuel cell system of the commercial FCV considering homogenous (A) and heterogenous heat and mass transfer (B).

following section. Moreover, by this point, it can be highlighted that the maximum power by itself does demonstrate if the fuel cell would be a better choice than another. For example, sample E2 - 3.5 Pt can reach a higher maximum power compared to sample E1 - 3.3 Pt, thus, requiring fewer cells to meet the same power as the commercial FCV. However, as previously shown in Fig. 4, sample E1 has higher efficiency for most of the power range indicating its higher performance for a specific power range without reaching the same maximum power. For the same maximum power, sample E1 compared to sample E2 shows a higher efficiency for the whole power range considered but with 40% more cells. Therefore, understanding the application operation range is highly relevant to scaling up the fuel cell as well as to determining whether one fuel cell fits better than another. The fuel cell loss contribution will be introduced in the next section along with each vehicle powertrain loss

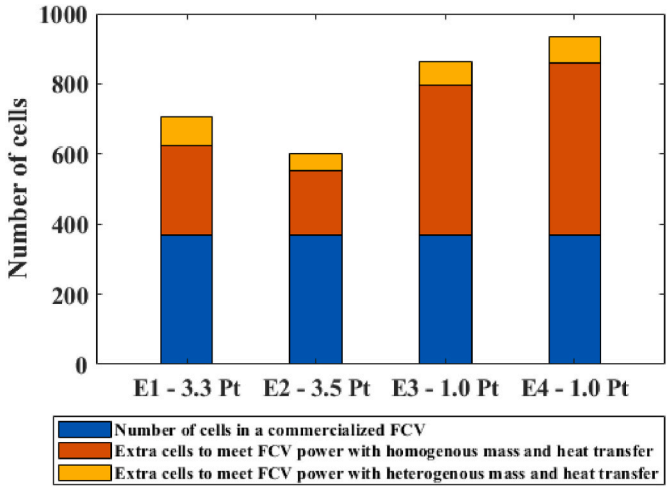

Fig. 5. The number of single cells needed for the samples E1-E4 with low and ultra-low Pt loading catalysts for fuel cell systems of 114 kW maximum power.

contribution.

3.3. Powertrain component loss contribution

The energy loss contribution for each powertrain component in kWh/km is described in Table 2. Besides the wheels (car model demand), gear, motor and inverter, battery, and fuel cell system, there were also losses related to the battery's maximum charging rate (braking energy loss). Those losses correspond to the energy that could not be stored in the battery when the braking energy was higher than the maximum charging rate of the battery. These losses could be avoided by using a bigger battery, or a higher performance power optimized battery and it should be the trend for the next generation fuel cell vehicles. Meanwhile, the maximum power of the battery did not add extra losses to the system because the discharging rate was higher compared to the charging, as well as the fact that the fuel cell would cover the extra power needed. As shown in Fig. 7, the power coming from the battery (positive power) is limited by its maximum power (24 kW) while the power coming into the battery (negative power) was lower due to higher limitation in its charging rate which caused loss regarding braking energy recovery.

Likewise, the fuel cell minimum power did not add extra losses because the extra power would be too short, or the battery could store the extra power. Regarding the battery loss itself, it can be observed that this is the most efficient component presenting the lowest loss in the system. This is followed by the gear and the motor with the inverter. When it comes to the fuel cell system, the losses naturally reach higher values, being the main source of losses in the system. Thus, this component is the one that most affects the overall efficiency as will be discussed in the following section. Since for all the models proposed here, the components were the same except for the fuel cell, the losses for each component excluding the fuel cell were also the same. The fuel cell system losses for both cases and each of the materials will be further detailed in the next section.

Table 2
Component loss contribution in the WLTP drive cycle.

Component	E (kWh/km)
Wheels	0.1154
Gear	0.0065
Motor + Inverter	0.0164
Battery	0.0049
Braking energy not recovered	0.0084
Fuel cell losses	0.0466–0.0619
Total	0.1986–0.2139

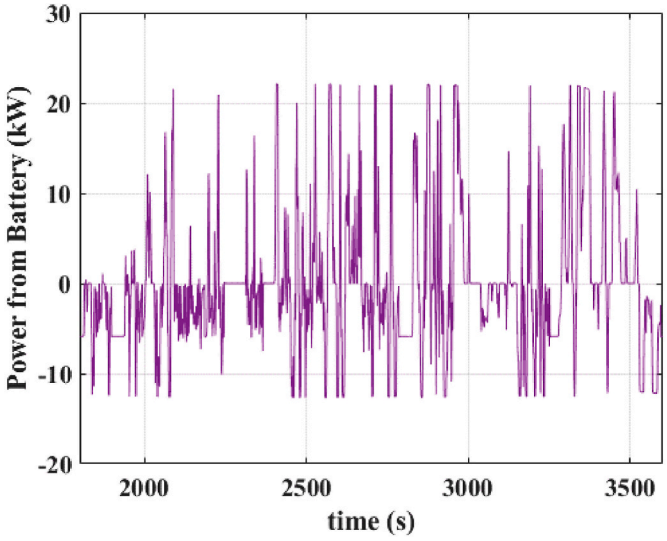

Fig. 7. Power from the battery in kW related to the time corresponding to the second simulated cycle (WLTP driving cycle as reference).

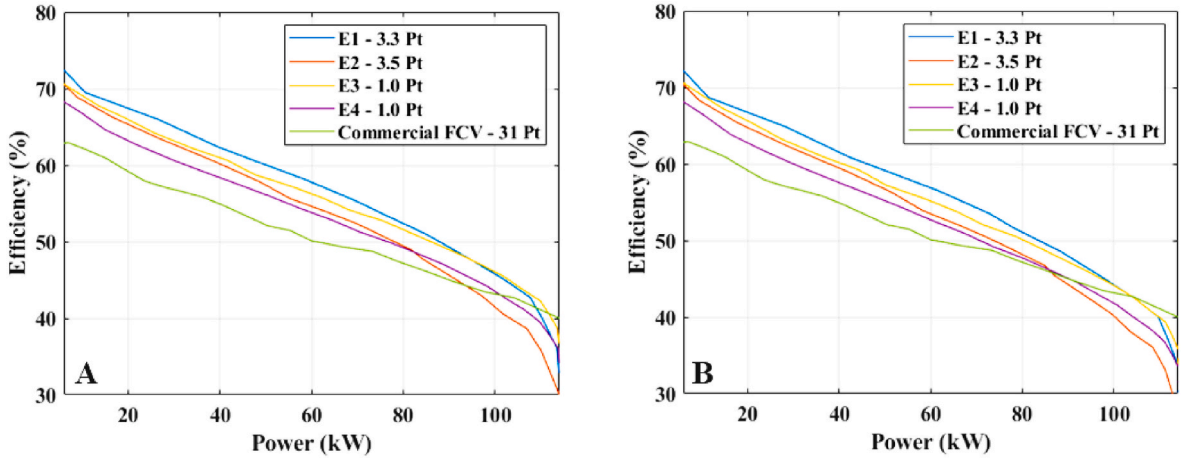

Fig. 6. Fuel cell systems of 114 kW maximum power of the single cell samples E1-E4 with low and ultra-low Pt loading compared with the fuel cell system of the commercial FCV considering homogenous (A) and heterogenous heat and mass transfer (B).

3.4. Fuel cell load and losses

The fuel cell load for all the models was the same since all the other components besides the fuel cell were the same. Thus, the fuel cell power that each fuel cell system must deliver was the same, however, the losses that each system generated were different according to its power-efficiency curve. As can be seen in Fig. 8, the power requirement from the fuel cell is always lower than 40 kW. These results agree with previous reports that found that commercial FCVs operate with a power of up to 40 kW in the motorway section [31,32]. Thus, when it comes to commercial FCVs, it can be noticed that the fuel cell is oversized compared to the vehicle power requirement. In this regard, while the considered commercialized FCV has a maximum power of 114 kW, the power requirement from the fuel cell is never higher than 40 kW at any driving cycle point. Two reasons that could be related to this choice are the safety to ensure that the fuel cell operation could be much higher if needed, and mostly to force the fuel cell operation into high-efficiency regions. Thus, considering this oversizing strategy, regarding scaling up from single fuel cell results to vehicle application, the most relevant part of the curve is its peak efficiency and the curve profile up to 40 kW which makes the analyzed fuel cell systems promising compared to the commercial one.

Therefore, since the single cells comprising low-loading Pt selected in this work show high efficiency operating at low power, as shown in Fig. 6A, they seem to be an attractive alternative for commercial fuel cells. For model 2, all the systems comprising ultra-low and low-loading Pt are promising, since they have shown higher efficiency for the fuel cell power operating range during the driving cycle, as previously shown in Fig. 6B. As a result, for model 1 where all the systems have the same number of cells, the fuel cell systems composed of samples E1 - 3.3 Pt and E2 - 3.5 Pt showed a fuel cell system efficiency of 64–66% for the driving cycle, while for the commercial FCV, the value was 61%. Those efficiencies corresponded to 0.0466–0.0539 kW h/km of fuel cell losses for samples E1 and E2, and 0.0583 kW h/km for the commercial system previously shown in Table 2. Thus, the total powertrain car efficiency of 56–58% found for the systems composed of low-loading Pt catalyst was higher compared to 55% for the commercial FCV. This higher efficiency is reflected in a higher driving range for vehicles comprising E1-E2 in the range of 641–651 km for samples E1-E2 while the commercial FCV was 628 km, considering a 4 kg hydrogen tank and a hydrogen energy content of 33 kW h/km. Meanwhile, the fuel cell systems composed of ultra-low Pt loading cells showed similar/slightly higher efficiency with sample E3 -1.0 Pt and slightly lower efficiency 58–60% efficiency with sample E4 - 1.0 Pt. Those efficiencies were related to 0.0483–0.0619 kW h/km fuel cell losses shown in Table 2, leading to a similar total powertrain car efficiency, 54–56%, and a similar driving range, 617–632 km, compared to the commercial FCV. These results indicate the potential of reducing the amount of platinum mass for FCVs by 89–97%, impacting about 31–45% of the total fuel cell cost, without compromising their efficiency. Overall, combining the results of the fuel cell power-efficiency curves (Fig. 4) and the results of the fuel cell demand (Fig. 8) is evident that FCVs composed of samples E1-E2 can reach high efficiencies for the whole driving cycle, while samples E3-E4 start to have their efficiency compromised at high-speed-regions. These results indicate that vehicles composed of samples E3-E4 would have their performance limited on the highway, requiring, in that case, high-power fuel cell stacks to achieve high efficiencies, as further addressed in model 2.

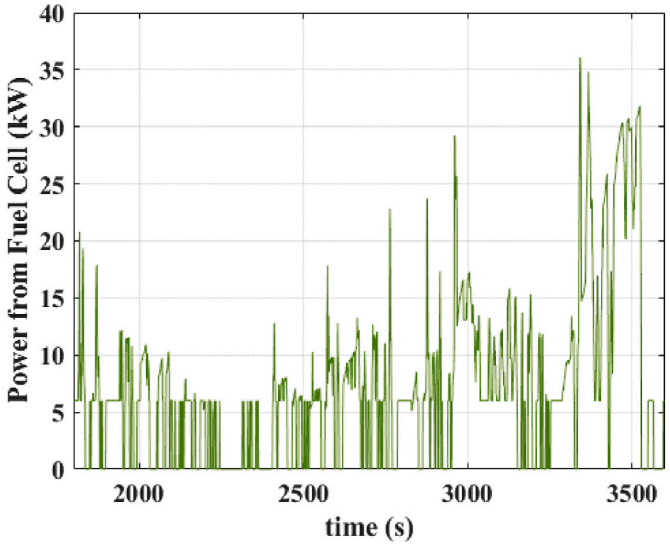

Fig. 8. Power from the fuel cell in kW related to the time corresponding to the second simulated cycle (WLTP driving cycle as reference).

Regarding model 2, where the fuel cells were scaled up for the same maximum power of a commercial FCV, efficiencies even higher were found for all the FCVs comprising ultra-low and low-loading platinum catalysts. For all the samples, fuel cell efficiencies in the range of 66–69% were achieved, reflecting powertrain efficiencies of 56–58%, and a driving range of 646–665 km. In this case, even though more cells are needed, those systems would still represent a reduction of 81% of the total Pt loading compared to the commercial FCV. This Pt mass reduction can impact a cost reduction of at least 27% in fuel cell cost, considering that the cathode corresponds to 85% of the total cathode Pt loading. Thus, oversizing systems composed of single fuel cells with ultra-low and low loading Pt loading could be a promising strategy both to move the system operation to more stable regions regarding power variation as well as to improve the system efficiency. The calculated efficiencies and driving range for models 1 and 2 are summarized in Table 3.

3.5. Analysis limitations

The scale-up analysis proposed here for the system and heat and mass transfer has considered losses based on previously reported data. However, these losses, related to the temperature distribution and water and oxygen transportation, might be different for the materials considered here. Nevertheless, since those losses are more significant for higher power, it can be assumed that the current analysis is reasonably representative. The same relation can be inferred for model 2, where the losses related to the addition of other components besides the cells were not considered. These losses would be more relevant for higher power applications and regarding costs, platinum is still considered the bottleneck of the device cost. Increasing the number of cells should also affect the space required for the fuel cell stack in the vehicle. Even though this constraint implication could not be evaluated in the present work, this should be considered in the engineering layout of FCVs comprising low-loading Pt catalysts with higher maximum power (>80 kW). Concerning this work, if the vehicle space needed could be addressed, these fuel cells could significantly reduce the amount of platinum while increasing the vehicle efficiency. Regarding extending the analysis from this work to other vehicle types some aspects should be acknowledged. Even though oversizing the fuel cell is already a strategy used for commercial FCVs, this strategy surely comes with costs, and it is hardly applicable for other vehicle types, such as plug-in vehicles, where the fuel cell is not the only main energy source. To address all these issues experimental scaling-up analysis of emerging high-performance nanotechnologies should be a matter of future investigation. Concerning this work, we have demonstrated a promising direction for the reduction of Pt content in the FCV system for a driving cycle supporting an energy transition based on hydrogen as well as assisting future studies and decision makers regarding clean transportation options.

Table 3
Efficiencies of the fuel cell system, powertrain efficiency, and vehicle driving range for models 1 and 2 considering the FCV comprising low-loading Pt fuel cell systems (E1-E4) or commercial Pt-loading fuel cell systems.

	E1	E2	E3	E4	Commercial
Pt loading (mg/cm^2)	0.033	0.035	0.01	0.01	0.31
Model 1					
Number of cells	370	370	370	370	370
Maximum Power (kW)	62–68	70–77	48–53	45–49	114
Fuel cell efficiency (%)	64.5–65.8	63.7–64.8	61.6–62.9	58.2–59.7	60.7
Vehicle efficiency (%)	56.4–56.9	56.1–56.2	55.2–55.8	53.9–54.5	54.9
Vehicle range (km)	646–651	641–646	632–638	617–623	628
Model 2					
Number of cells	623–677	552–600	795–864	860–935	370
Maximum Power (kW)	114	114	114	114	114
Fuel cell efficiency (%)	68.1–68.6	66.4–66.9	67.1–67.4	64.6–65.0	60.7
Vehicle efficiency (%)	57.9–58.1	57.2–57.4	57.5–57.6	56.5–56.6	54.9
Vehicle range (km)	662–665	654–656	632–638	646–647	628

4. Conclusion

In this work, novel low-loading Pt fuel cell catalysts were scaled up, and simulated to a driving cycle and their performance was compared to a commercial FCV. Some main conclusions of this work can be summarized as follows.

- When scaling up from single cells to stack and systems, the fuel cells comprising low Pt-loading presented a higher variation in efficiency compared to a fuel cell from a commercial FCV. This higher declination in the fuel cell efficiency curve profile can be possibly associated with the lower content of platinum which leads to a lower maximum power capacity.
- Even though the fuel cells comprising low-loading Pt present a less stable profile compared to the fuel cell from the commercial FCV, the average fuel cell efficiencies during the investigated driving cycle using the same number of cells were higher or just slightly worse/similar if compared to the commercial FCV due to their higher efficiencies at low power.
- When the cells were scaled up for the same power as the fuel cell from the commercial FCV, all the low-loading Pt fuel cells investigated presented at least 4% higher efficiency compared to the one from the commercial FCV. In this case, more cells are needed, however, the amount of Pt is at least 81% lower compared to the commercial amount, which can reduce the fuel cell cost by at least about 27%.
- Although maximum power capacity is a relevant parameter to take into consideration for scaling up single fuel cells to stack and systems, performing efficiently at lower power can bring low-loading Pt catalysts closer to FCV applications if making sure they are scaled up enough to perform at higher efficiencies. This seems to be more relevant to material development than just comparing the highest power the catalyst can reach. This oversized strategy is already used for the current commercial FCVs to keep the fuel cell operation at high efficiency.

CRediT authorship contribution statement

Tatiana Santos Andrade: Writing – original draft, Methodology, Investigation. **Torbjörn Thiringer:** Writing – review & editing, Supervision, Funding acquisition.

Declaration of competing interest

No conflict of interest

Data availability

Data will be made available on request.

Acknowledgments

The authors acknowledge the financial support from Chalmers' Area of Advance Transport.

References

[1] O. Lori, L. Elbaz, Recent advances in synthesis and utilization of ultra-low loading of precious metal-based catalysts for fuel cells, ChemCatChem 12 (2020) 3434–3446, https://doi.org/10.1002/cctc.202000001.
[2] S. Liu, S. Yuan, Y. Liang, H. Li, Z. Xu, Q. Xu, et al., Engineering the catalyst layers towards enhanced local oxygen transport of Low-Pt proton exchange membrane fuel cells: materials, designs, and methods, Int. J. Hydrogen Energy 48 (2023) 4389–4417, https://doi.org/10.1016/j.ijhydene.2022.10.249.
[3] L. Osmieri, J. Park, D.A. Cullen, P. Zelenay, D.J. Myers, K.C. Neyerlin, Status and challenges for the application of platinum group metal-free catalysts in proton-exchange membrane fuel cells, Curr. Opin. Electrochem. 25 (2021), https://doi.org/10.1016/j.coelec.2020.08.009.
[4] U.S.DRIVE Fuel Cell Tech Team, DOE technical targets for polymer electrolyte membrane fuel cell components. https://www.energy.gov/eere/fuelcells/doe-technical-targets-polymer-electrolyte-membrane-fuel-cell-components, 2017, 1–8.
[5] L. Pan, S. Ott, F. Dionigi, P. Strasser, Current challenges related to the deployment of shape-controlled Pt alloy oxygen reduction reaction nanocatalysts into low Pt-loaded cathode layers of proton exchange membrane fuel cells, Curr. Opin. Electrochem. 18 (2019) 61–71, https://doi.org/10.1016/j.coelec.2019.10.011.
[6] J. Fan, M. Chen, Z. Zhao, Z. Zhang, S. Ye, S. Xu, et al., Bridging the gap between highly active oxygen reduction reaction catalysts and effective catalyst layers for proton exchange membrane fuel cells, Nat. Energy 6 (2021) 475–486, https://doi.org/10.1038/s41560-021-00824-7.
[7] Y. Wang, D.F. Ruiz Diaz, K.S. Chen, Z. Wang, X.C. Adroher, Materials, technological status, and fundamentals of PEM fuel cells – a review, Mater. Today 32 (2020) 178–203, https://doi.org/10.1016/j.mattod.2019.06.005.
[8] Y. Wang, H. Yuan, A. Martinez, P. Hong, H. Xu, F.R. Bockmiller, Polymer electrolyte membrane fuel cell and hydrogen station networks for automobiles: status, technology, and perspectives, Adv. Appl. Energy 2 (2021), https://doi.org/10.1016/j.adapen.2021.100011.
[9] Y. Shao, J.P. Dodelet, G. Wu, P. Zelenay, PGM-free cathode catalysts for pem fuel cells: a mini-review on stability challenges, Adv. Mater. 31 (2019), https://doi.org/10.1002/adma.201807615.
[10] A. Uddin, L. Dunsmore, H. Zhang, L. Hu, G. Wu, S. Litster, High power density platinum group metal-free cathodes for polymer electrolyte fuel cells, ACS Appl. Mater. Interfaces 12 (2020) 2216–2224, https://doi.org/10.1021/acsami.9b13945.
[11] K. Kodama, T. Nagai, A. Kuwaki, R. Jinnouchi, Y. Morimoto, Challenges in applying highly active Pt-based nanostructured catalysts for oxygen reduction reactions to fuel cell vehicles, Nat. Nanotechnol. 16 (2021) 140–147, https://doi.org/10.1038/s41565-020-00824-w.
[12] Y.J. Lee, H.E. Kim, E. Lee, J. Lee, S. Shin, H. Yun, et al., Ultra-low Pt loaded porous carbon microparticles with controlled channel structure for high-performance fuel cell catalysts, Adv. Energy Mater. 11 (2021), https://doi.org/10.1002/aenm.202102970.
[13] L. Chong, J. Wen, J. Kubal, F.G. Sen, J. Zou, J. Greeley, et al., Ultralow-loading platinum-cobalt fuel cell catalysts derived from imidazolate frameworks, Science 362 (2018) 1276–1281, https://doi.org/10.1126/science.aau0630, 80-.
[14] R.K. Ahluwalia, X. Wang, J.-K. Peng, V. Konduru, S. Arisetty, N. Ramaswamy, et al., Achieving 5,000-h and 8,000-h low-PGM electrode durability on automotive drive cycles, J. Electrochem. Soc. 168 (2021) 044518, https://doi.org/10.1149/1945-7111/abf507.
[15] H. Lohse-Busch, K. Stutenberg, M. Duoba, X. Liu, A. Elgowainy, M. Wang, et al., Technology Assessment of a Fuel Cell Vehicle, US DOE -Energy Syst Div, 2017.
[16] H. Lohse-Busch, K. Stutenberg, M. Duoba, X. Liu, A. Elgowainy, M. Wang, et al., Automotive fuel cell stack and system efficiency and fuel consumption based on

vehicle testing on a chassis dynamometer at minus 18 °C to positive 35 °C temperatures, Int. J. Hydrogen Energy 45 (2020) 861–872, https://doi.org/10.1016/j.ijhydene.2019.10.150.
[17] J. Wang, Barriers of scaling-up fuel cells: cost, durability and reliability, Energy 80 (2015) 509–521, https://doi.org/10.1016/j.energy.2014.12.007.
[18] H. Onggo, Y. Irmawati, R. Yudianti, Comparative studies on performance of single cell and PEMFC stack, AIP Conf. Proc. 1711 (2016), https://doi.org/10.1063/1.4941636.
[19] C. Bonnet, S. Didierjean, N. Guillet, S. Besse, T. Colinart, P. Carré, Design of an 80kWe PEM fuel cell system: scale up effect investigation, J. Power Sources 182 (2008) 441–448, https://doi.org/10.1016/j.jpowsour.2007.12.100.
[20] J.P. Hensel, R.S. Gemmen, J.D. Thornton, J.S. Vipperman, W.W. Clark, B.A. Bucci, Effects of cell-to-cell fuel mal-distribution on fuel cell performance and a means to reduce mal-distribution using MEMS micro-valves, J. Power Sources 164 (2007) 115–125, https://doi.org/10.1016/j.jpowsour.2006.09.049.
[21] H. Leelasupakorn, A. Kaewchada, W. Traisantikul, W. Tiengtrakarnsuk, S. Limtrakul, T. Vatanatham, Scaleup effect on performance of proton exchange membrane fuel cell, Chiang Mai J. Sci. 35 (2008) 89–94.
[22] M. Miller, A. Bazylak, A review of polymer electrolyte membrane fuel cell stack testing, J. Power Sources 196 (2011) 601–613, https://doi.org/10.1016/j.jpowsour.2010.07.072.
[23] WLTPfactseu. What Is WLTP and How Does it Work? n.d..
[24] T.S. Andrade, T. Thiringer, From hydrogen fuel to wheels: characterizing the powertrain hydrogen/energy consumption for battery versus hydrogen fuel cell vehicle, in: 2023 IEEE IAS Glob Conf Renew Energy Hydrog Technol GlobConHT 2023, 2023, https://doi.org/10.1109/GlobConHT56829.2023.10087509.
[25] E. Wikner, Ageing in Commercial Li-Ion Batteries : Lifetime Testing and Modelling for Electrified Vehicle Applications, 2019.
[26] E. Wikner, E. Björklund, J. Fridner, D. Brandell, T. Thiringer, How the utilised SOC window in commercial Li-ion pouch cells influence battery ageing, J. Power Sources Adv. 8 (2021), https://doi.org/10.1016/j.powera.2021.100054.
[27] Hyundai, Hyundai Ix35 Fuel Cell, Press Releases, 2013, p. 1.
[28] LithiumWerks, Lithium-ion 18650 Power Cells 1–7 (2023).
[29] A. Kongkanand, M.F. Mathias, The priority and challenge of high-power performance of low-platinum proton-exchange membrane fuel cells, J. Phys. Chem. Lett. 7 (2016) 1127–1137, https://doi.org/10.1021/acs.jpclett.6b00216.
[30] A. Ganeşan, M. Narayanasamy, Ultra - Low Loading of Platinum in Proton Exchange Membrane - Based Fuel Cells : a Brief Review, 2020.
[31] I. Pielecha, Modeling of fuel cells characteristics in relation to real driving conditions of FCHEV vehicles, Energies 15 (2022), https://doi.org/10.3390/en15186753.
[32] I. Pielecha, A. Szałek, G. Tchorek, Two generations of hydrogen powertrain — an analysis of the, Energies 15 (2022) 1–20.